Edinburgh Research Explorer

Target-oriented Marchenko imaging of a North Sea field

Target-oriented Marchenko imaging of a North Sea field

Matteo Ravasi[1], Ivan Vasconcelos[2], Alexander Kritski[3],

Andrew Curtis[4], Carlos Alberto da Costa Filho[4], Giovanni Angelo Meles[4]

[1]Presently Statoil ASA, Bergen, Norway. Formerly, School of GeoSciences, The
University of Edinburgh, Edinburg, United Kingdom.

[2]Schlumberger Gould Research, Cambridge, United Kingdom.

[3]Statoil ASA, Trondheim, Norway.

[4]School of GeoSciences, The University of Edinburgh, Edinburg, United Kingdom.

Corresponding author: Matteo Ravasi (*M.Ravasi@sms.ed.ac.uk*)

Running head: Marchenko imaging of a North Sea field

Estimate Word count: 3301 + 300*5 (Figures) = 4801

Abstract

Seismic imaging provides much of our information about the Earth's crustal structure. The principal source of imaging errors derives from simplistic modelled predictions of the complex, scattered wavefields that interact with each subsurface point to be imaged. A new method of wavefield extrapolation based on inverse scattering theory in mathematical physics produces accurate estimates of these subsurface scattered wavefields, while still using relatively little information about the Earth's properties. We use it for the first time to create real target-oriented seismic images of a North Sea field. We synthesise underside illumination from surface reflection data, and use it to reveal subsurface features that are not present in an image from conventional migration of surface data. To reconstruct underside reflections, we rely on the so-called downgoing focusing function, whose coda consists entirely of transmission-born multiple scattering. As such, with the method presented here, we provide the first field data example of reconstructing underside reflections with contributions from transmitted multiples, without the need to first locate or image any reflectors in order to reconstruct multiple scattering effects.

Keywords

1. Introduction

Imaging the geometry and properties of complex subsurface geology, identifying and characterizing subsurface reservoirs of hydrocarbons, minerals or water, as well as monitoring of waste products stored underground such as CO_2 and nuclear waste, all require sophisticated seismic imaging and monitoring. A crucial step for such imaging methods is the estimation of wavefields within the solid Earth's interior where no direct observations are available. Standard estimation or 'redatuming' approaches based on time-reversal of data recorded along an open boundary of surface receivers (Berryhill, 1984) generally fail to explain how energy propagates in the complex subsurface unless high-resolution seismic velocity models are available *prior to* imaging as otherwise they can not accurately predict multiply scattered waves (multiples) in the subsurface. This causes large errors in images and, crucially, in interpretation.

Marchenko redatuming (or autofocusing) is a novel technique to estimate acoustic wavefields within the subsurface including primary and multiple reflections, using seismic waves measured at the Earth's surface and only a smooth estimate of the propagation velocity model (Rose, 2002; Broggini et al., 2012; Wapenaar et al., 2013). Advantages over standard redatuming methods are that the multiply-scattered wavefield coda is estimated at each subsurface image point, spurious arrivals due to multiples in the overburden are attenuated, and the retrieved wavefields are naturally separated into their up- and down-going components. The acoustic (fluid) theory was extended to elastic (solid) media by da Costa Filho et al. (2014) and Wapenaar (2014a), and the elastic imaging by da Costa Filho et al. (2015).

Standard migration techniques generate spurious structures in images as they do not correctly account for internal reflections (Malcolm et al., 2007). By contrast, Marchenko wavefields account for all multiples and Broggini et al. (2014), Behura et al. (2014) and Slob et al. (2014) construct synthetic images free from internal multiple artifacts by cross-correlating (or deconvolving) the retrieved up- and down-going fields at any subsurface image point. Wapenaar et al. (2014b) limit the computation of Marchenko fields to a single depth level, then use multi-dimensional deconvolution (Wapenaar et al., 2011; van der Neut & Herrmann, 2013) to create redatumed reflection responses from and to that depth, which are free of spurious events related to internal multiples in the overburden. These responses can be used for imaging target areas of the subsurface below or above the depth level of interest. Such images should be more accurate than those generated by standard reverse-time redatuming followed by cross-correlation of the subsurface responses (Dong et al., 2009) as overburden multiples are removed.

This paper presents the first successful application of target-oriented imaging using Marchenko redatuming on real field data. We apply the method to reflection seismic data recorded on an ocean-bottom cable (OBC) dataset over the Volve oilfield, offshore Norway in 2002. One of the main obstacles to the application of such novel techniques to field datasets is the set of requirements of the reflection data (explained below). We show that a wave-equation method to redatum marine sources to the seabed, sea surface multiple removal, and seismic source signature removal, transforms ocean-bottom data into a suitable estimate of the reflection response required by the Marchenko scheme. We then produce images of target areas of shallow and deep subsurface

structures using Marchenko wavefields, and compare these to images obtained from standard reverse-time migration (RTM) of the same surface data.

2. Marchenko equations

Marchenko redatuming is based on two wave states which uniquely relate subsurface wavefields from surface sources to so-called focusing functions via the recorded seismic data (Wapenaar et al., 2014b). The subsurface wavefields ($\mathbf{g}^-$ and $\mathbf{g}^+$) belong to the wave state of the physical world in which data are acquired, while the focusing functions ($\mathbf{f}^-$ and $\mathbf{f}^+$) are defined in a modified medium that is homogeneous below a chosen subsurface level. These are related by (van der Neut et al., 2014)

$$\mathbf{g}^- = \mathbf{R}\mathbf{f}^+ - \mathbf{f}^-$$

$$\mathbf{g}^{+*} = -\mathbf{R}^*\mathbf{f}^- + \mathbf{f}^+ \tag{1}$$

Here $\mathbf{g}^-$ and $\mathbf{g}^+$ are matrices containing the time-space domain up- and down-going Green's functions, with multiple sources at the acquisition surface and receivers located at a desired subsurface point. The focusing functions $\mathbf{f}^-$ and $\mathbf{f}^+$ are respectively up- and down-going acausal solutions to the wave-equation that focus at zero-time at the same subsurface point, and then continue as down-going diverging fields into the homogeneous lower half-space. We suppose that $\mathbf{f}^+ = \mathbf{f}_d^+ + \mathbf{f}_m^+$, that is, $\mathbf{f}^+$ is composed of a direct wave $\mathbf{f}_d^+$ followed by a coda $\mathbf{f}_m^+$: these quantities are also organized in matrices with concatenated traces in the time-space domain. Matrix $\mathbf{R}$ contains the real Earth's reflection response from vertical dipole sources to pressure receivers, and left-multiplication is equivalent to performing multi-dimensional convolution in the time-space domain,

while ***** acts on a matrix by time reversing its traces.

To obtain a system of coupled Marchenko equations, a muting function Θ that removes the direct arrival and all subsequent events is defined. Assuming that the muting function satisfies $\Theta \mathbf{g}^- = 0$, $\Theta \mathbf{g}^+ = 0$, $\Theta \mathbf{f}^+ = \mathbf{f}_m^+$, and $\Theta \mathbf{f}^- = \mathbf{f}^-$ (Wapenaar et al., 2014b), its application to equations 1 yields

$$\mathbf{f}^- = \Theta \mathbf{R} \mathbf{f}_d^+ + \Theta \mathbf{R} \mathbf{f}_m^+$$

$$\mathbf{f}_m^+ = \Theta \mathbf{R}^* \mathbf{f}^- . \tag{2}$$

Starting from an initial focusing function $\mathbf{f_d}^+$, obtained by inverting (or time-reversing) an estimate of the direct wave $\mathbf{G_d}$ from the subsurface point to the surface and assuming a null coda ($\mathbf{f_m}^+ = 0$), equations 2 can be iterated to convergence. As noted by van der Neut et al. (2015) and Vasconcelos et al. (2015), the solution of the focusing functions at the iteration K can be written in a compact form by means of a Neumann series expansion:

$$\mathbf{f}^{+(K)} = \sum_{k=0}^{K} (\Theta \mathbf{R}^* \Theta \mathbf{R})^k \mathbf{f}_d^+$$

$$\mathbf{f}^{-(K)} = \Theta \mathbf{R} \sum_{k=0}^{K} (\Theta \mathbf{R}^* \Theta \mathbf{R})^k \mathbf{f}_d^+ . \tag{3}$$

where each term in the series represents an update to the focusing function. Finally, up- and down-going Green's function can be computed from equations 1 using the estimated focusing functions $\mathbf{f}^-$ and $\mathbf{f}^+$. These Green's functions are used to redatum the surface data to the subsurface points without knowledge of the intervening medium, and then to image the medium using reverse-time migration.

6

3. Marchenko inputs and redatumed fields

Marchenko redatuming requires certain characteristics of the reflection response $\mathbf{R}$. $\mathbf{R}$ is assumed to have been obtained from large aperture, fixed receiver arrays with dense source coverage coinciding with the entire receiver array, to have broad bandwidth, and to contain only primary reflections and internal multiples (i.e., is deprived of direct waves, source and receiver ghosts, and surface-related multiples). Recorded reflection data therefore approximate $\mathbf{R}$ only after pre-processing.

If data are acquired with standard ocean-bottom acquisition systems, wave-equation approaches to joint source redatuming (to the receiver level), demultiple, and source designature (Ziolkowski et al., 1999; Amundsen, 2001) can transform recorded data into a suitable estimate of reflection response $\mathbf{R}$. The essence of these methods is to solve the following frequency-space domain, integral relation by means of multi-dimensional deconvolution (*Wapenaar et al.*, 2011)

$$\mathbf{p}^- = \mathbf{R}\mathbf{p}^+ \tag{4}$$

where the recorded up-going decomposed data ($\mathbf{p}^-$) is seen as the result of multi-dimensional convolution of the down-going data ($\mathbf{p}^+$) and the desired reflection response ($\mathbf{R}$) that would be recorded in a hypothetical seismic experiment with no sea surface present. The decomposed data $\mathbf{p}^-$ and $\mathbf{p}^+$ are arranged in matrices containing responses from multiple sources to receivers at the acquisition surface. The sought reflection response $\mathbf{R}$ is also a matrix with responses from vertical particle velocity receivers to monopole virtual sources at the acquisition surface. Each frequency is inverted separately and the time-space response $\mathbf{R}$ is obtained by combining solutions of each

inversion via an inverse Fourier transform. Moreover, source-receiver reciprocity is applied to the retrieved response to obtain a reflection response from vertical dipole sources to pressure receivers as required from the theory of Marchenko redatuming.

For our current study, we use data from an ocean-bottom cable on the seabed above the Volve field located in the gas/condensate-rich Sleipner area of the North Sea, offshore Norway. The receiver line contains 235 receivers spaced 25 m apart, and an overlying shot line of 241 sources spaced 50 m apart, as shown in Figure 1a. Noise suppression, vector-fidelity corrections, and initial source designature are applied to the data. Further, we scale the data by $\sqrt{t}$ to account for 3D geometrical spreading and we calibrate the direct arrival of the particle velocity measurement to the pressure recording [see also Ravasi et al., (2014)]. After wavefield separation is carried out in the frequency-wavenumber domain (Amundsen, 1993), the up- (Figure 1b) and down-going (Figure 1c) components are used as input for multi-dimensional deconvolution (equation 4), producing an estimate of the reflection response $\hat{\mathbf{R}}$ for Marchenko redatuming (Figure 1d). Standard reverse-time migration of $\hat{\mathbf{R}}$ (i.e., the up-going wavefield without source and receiver ghosts and free-surface multiples) is shown in Figure 2 for comparison with Marchenko imaging.

An estimate of the direct wavefront $\mathbf{G_d}$ is also required to create the initial focusing function $\mathbf{f_d}^+$. This can be computed by forward modeling (e.g., ray-tracing, finite-differences) using a smooth velocity model such as that shown in Figure 1a. For illustration, we compute the traveltime of the first arriving wave from a subsurface point $\mathbf{x_F}=\{6, 3.3\}$km by ray-tracing, then apply a 40Hz Ricker wavelet with constant amplitude for all offsets (Figure 3a). Focusing functions $\mathbf{f^+}$ and $\mathbf{f^-}$ estimated

after two iterations of the Marchenko equations ($K=2$ in equation 3) are shown in Figures 3b, c and are used in equations 1 to compute Green's functions $\mathbf{g}^+$ and $\mathbf{g}^-$ (Figures 3d,e). Note that the iterative Marchenko scheme has retrieved the coda in the down-going field: a wave with similar move-out to the direct arrival is visible at zero-offset around 1.5s in Figure 3d, which may have experienced multiple bounces in the high velocity layer in between 2.6 and 2.85 km depth.

A concern about the application of Marchenko redatuming to a field datasets is whether the iterative scheme presented above converges. Since we do not have direct access to the real Earth's reflection response $\mathbf{R}$, it is inevitable that the processed version of the recorded data $\hat{\mathbf{R}}$ will be scaled, such that $\hat{\mathbf{R}} = c_R \mathbf{R}$. Here c_R is at best an unknown scalar (or, more likely, a compact filter varying in time and space) that depends on the acquisition and processing chain. In this application, we have taken advantage of the observation that $\left| (\Theta \hat{\mathbf{R}}^* \Theta \hat{\mathbf{R}})^k \mathbf{f}_d^+ \right|^2 \rightarrow 0$ as $k \rightarrow \infty$ needs to hold for the Neumann series in equation 3 to converge (see Supporting Material). While meeting this condition does not guarantee that each update has the correct amplitude and may not allow complete cancellation of spurious arrivals in the up-going field, we show here that after two iterations of the Marchenko scheme this method produces a coda in the down-going focusing function (Figure 3b) and Green's function (Figure 3d) with non-negligible amplitudes.

An accurate deconvolution of the source wavelet from the data is however required for a correct summation of various updates of the Neumann series. In fact, each iteration of the Marchenko scheme involves one convolution and one correlation with reflection response $\hat{\mathbf{R}}$ to obtain $\mathbf{f}^+$, and a further convolution to construct $\mathbf{f}^-$ (equation 3): an unbalanced frequency response

may enhance some frequencies relative to others, rendering the focusing function updates from different iterations incompatible. In this study we attempted to remove the effect of the source signature from the data using the wave-equation demultiple approach of Amundsen (2001). While it is not possible to directly verify that the source wavelet has been fully deconvolved from the reflection data $\hat{\mathbf{R}}$, we note that that the original up-going data shows a much higher energy content at low frequencies (see insert in Figure 1b) while the reflection response obtained from multidimensional deconvolution has a better equalized amplitude spectrum (see insert in Figure 1a). It is finally important to note that other factors such as frequency-dependent attenuation, imperfect deghosting, unaccounted-for 3D effects, or noise affect the quality of the updates, and an adaptive scheme may further improve the robustness of Marchenko redatuming (van der Neut et al., 2014).

4. Marchenko imaging

Marchenko redatuming was used to retrieve up- and down-going Green's functions for 151 subsurface points forming a 1.5 km wide array ranging from 6.7 km to 8.2 km horizontally, at a depth level of 2.5 km (lower target box in Figure 1a). From these fields we obtain an estimate of the reflection response from above the target ($\mathbf{R}_{\cup}$) as if both sources and receiver were located along the array of subsurface points, within a modified medium with the same properties as the physical medium below the array but which is homogeneous above. We do so by solving the following equation in the frequency domain by means of multi-dimensional deconvolution (*Wapenaar et al.* 2014b):

$$\mathbf{g}^{-} = \mathbf{g}^{+}\mathbf{R}_{\cup}. \tag{5}$$

10

The estimate of $\mathbf{R}_\cup$ for a source in the centre of the subsurface array is shown in Figure 4a. As discussed extensively in Wapenaar et al. (2014b), the redatumed reflection response can be used as input for standard imaging in a target zone just *below* the redatumed level (Figure 4c). Comparison with standard reverse-time migration of our estimate of $\hat{\mathbf{R}}$ shows that Marchenko imaging from above is able to produce an image of similar quality to that from RTM (Figure 4e), perhaps slightly improving the details between the main reflectors at 2.6 and 2.9 km, and limiting the required (expensive) finite-difference computation for RTM to a much smaller subsurface target zone.

The computational advantage already represents a reason to perform Marchenko imaging over standard RTM when we are interested in creating target-oriented images. However, the focusing functions $\mathbf{f}^-$ and $\mathbf{f}^+$ can also be combined to obtain a second estimate of the reflection response which illuminates the target area from below ($\mathbf{R}_\cap$) (Wapenaar et al., 2014b):

$$-\mathbf{f}^{-*} = \mathbf{f}^+\mathbf{R}_\cap. \tag{6}$$

The estimate of $\mathbf{R}_\cap$, shown in Figure 4b for a source in the centre of the subsurface array at a depth of 3.3 km, is used to image the target zone just *above* the lower redatumed level (Figure 4d) producing a similar image to panel c. Reflections $\mathbf{R}_\cap$ illuminating this portion of the subsurface from below contain complementary information to $\mathbf{R}_\cup$, at least when the lateral extension of the arrays of subsurface points used for imaging from above and below is the same. It is however important to note that the reflection $\mathbf{R}_\cap$ does not really contain information from the portion of the subsurface below the focusing level: this is because $\mathbf{R}_\cap$ originates from focusing functions belonging to a medium that is homogeneous below the focusing level (Wapenaar et al., 2015).

Similarly, Marchenko fields were computed along a line at 1.13 km depth (upper box in Figure 1a) to image the complex stratigraphy in the shallow subsurface from below (Figure 4f and g). Spatial aliasing occurs in the standard RTM image (Figure 4h) as this was originally sampled every 10m to save on computational cost. The Marchenko image may be sampled relatively cheaply every 5 m due to the limited area of required finite-difference modeling, and compares favorably to that from RTM.

Finally, Marchenko imaging from below is performed for two additional subsurface lines with inter-receiver spacing of 10 m: the first ranges from 5.4 km to 6.9 km horizontally at depth 3.4 km, while the second is at 3.41 km depth and extends from 4.1 km to 5.6 km horizontally. The resulting images are located either side of that in Figure 4d, and all three are merged to form Figure 5b. Note that since each of the reflection responses $\mathbf{R}_\cap$ is obtained using multi-dimensional deconvolution, the aperture of the subsurface array should not exceed that of sources at the acquisition surface for a successful inversion of equation 6. Additionally, sparse (rather than dense) subsurface points will result in spatial aliasing, making the inversion unstable. On the other hand, if the number of subsurface points is higher than that of sources at the acquisition surface, the solution of equation 6 would generally give rise to a less accurate response. With the choice of the extension and sampling of the subsurface array being limited by these constraints, it is important to assure that images obtained independently from different subsurface responses $\mathbf{R}_\cap$ at different depth levels can be combined together compatibly. Green arrows in Figure 5b indicate near-perfect continuity of reflectors between the various images, thus showing that we may design short-aperture, finely sampled subsurface arrays that prevent spatial aliasing in the subsequent imaging step. Finally,

Marchenko imaging from below reveals structural features (blue arrows in Figure 5b), which are not present in our surface RTM image of the reflection response $\hat{R}$ (Figure 5a). While our interpretation of these events is that of physical structures that are perhaps hidden under coherent noise in the RTM image, they could also represent artificial structure arising from a sub-optimal choice of the scaling c_R that over-predicts spurious events in the up-going field (see Supporting Material).

5. Conclusions

The novel technique of Marchenko redatuming applied to an ocean-bottom seismic data acquired over the Volve North Sea field, produces encouraging results of target-oriented imaging of both shallow and deep structures. Although a by-product of the information contained in the original data, Marchenko focusing functions also contain sufficient information to directly image the subsurface using reconstructed underside reflections. Such images seem to reveal coherent features beneath strongly reflecting interfaces, which are distorted or invisible when imaging directly with surface data. This coherency supports the observation that the information in the retrieved focusing functions recasts that in the original data in a manner which is both nontrivial and useful. As such, we envisage that other practices that require wavefield focusing such as microseismic source localization, seismic time-lapse monitoring, and non-destructive testing might also benefit from estimates of focusing functions obtained by Marchenko redatuming.

6. Acknowledgments

7. References

Amundsen, L., 1993. Wavenumber-based Filtering of Marine Point Source Data. Geophysics, 58 (9), 1335-1348. doi: 10.1190/1.1443516.

Amundsen, L., 2001. Elimination of free-surface related multiples without need of the source wavelet. Geophysics, 66(1), 327–341. doi: 10.1190/1.1444912.

Berryhill, J. R., 1984. Wave-equation datuming before stack. Geophysics, 49(11), 2064–2066. doi: 10.1190/1.1441620.

Behura, J., Wapenaar, K. & Snieder, R., 2014. Autofocus imaging: Image reconstruction based on inverse scattering theory. Geophysics, 79(3), A19-A26. doi: 10.1190/geo2013-0398.1.

Broggini, F., Snieder, R., & Wapenaar, K., 2012. Focusing the wavefield inside an unknown 1D medium: Beyond seismic interferometry. Geophysics, 77(5), A25-A28. doi: 10.1190/geo2012-0060.1

Broggini, F., Snieder, R., & Wapenaar, K., 2014. Data-driven wavefield focusing and imaging with multidimensional deconvolution: Numerical examples for reflection data with internal multiples: Geophysics, 79(3), WA107-WA115. doi: 10.1190/geo2013-0307.1.

Dong S., Y. Luo, X. Xiao, S. Chavez-Perez, & Schuster, G. T., 2009. Fast 3D target-oriented reverse-time datuming. Geophysics, 74(6), WCA141- WCA151. doi: 10.1190/1.3261746.

da Costa Filho, C.A., Ravasi, M., Curtis, A., & Meles, G.A., 2014. Elastodynamic Green's Function Retrieval through Single-Sided Marchenko Inverse Scattering. Physical Review Editions, 90, 063201. doi: 10.1103/PhysRevE.90.063201.

da Costa Filho, C.A., Ravasi, M., & Curtis, A., 2015. Elastic P and S wave autofocus imaging with primaries and internal multiples. Geophysics, In Press.

Malcolm, A. E., de Hoop, M. V., & Calandra, H., 2007. Identification of image artifacts from internal multiples: Geophysics, 72(2), S123–S132. doi: 10.1190/1.2434780.

van der Neut, J., & Herrmann, F., 2013. Interferometric redatuming by sparse inversion. Geophysical Journal International, 192, 666-670. doi: 10.1093/gji/ggs052.

van der Neut, J., Wapenaar, K., Thorbecke, J., & Vasconcelos, I., 2014. Internal multiple suppression by adaptive Marchenko redatuming. 84th annual SEG meeting, Technical Program Expanded Abstracts, 4055-4059. doi: 10.1190/segam2014-0944.1.

van der Neut, J., Vasconcelos, I. and Wapenaar, K., 2015. On Green's function retrieval by iterative substitution of the coupled Marchenko equations. Geophysical Journal International, 203, 792-813.

Ravasi, M., Vasconcelos, I., Curtis, A., & Kritski, A., 2014. Vector-Acoustic reverse-time migration of Volve OBC dataset without up/down decomposed wavefields. Second EAGE/SBGf Workshop.

Rose, J. H., 2002. Single-sided autofocusing of sound in layered materials. Inverse Problems, 18, 1923–1934. doi:10.1088/0266-5611/18/6/329.

Slob, E., Wapenaar, K., Broggini, F., & Snieder, R., 2014. Seismic reflector imaging using internal multiples with marchenko-type equations: Geophysics, 79(2), S63–S76. doi: 10.1190/geo2013-0095.1.

Vasconcelos, I., Wapenaar, K., van der Neut, J., Thomson, C., & Ravasi, M., 2015. Using inverse transmission matrices for Marchenko redatuming in highly complex media. 85th annual SEG meeting.

Wapenaar, K., 2014a. Single-sided Marchenko focusing of compressional and shear waves. Physical Review Edition, 90(6), 063202. doi: /10.1103/PhysRevE.90.063202.

Wapenaar, K., van der Neut, J., Ruigrok, E., Draganov, D., Hunziker, J., Slob, E., Thorbecke, J., & Snieder, R., 2011. Seismic interferometry by crosscorrelation and by multi-dimensional deconvolution: a systematic comparison. Geophysical Journal International, 185(3), 1335-1364. doi: 10.1111/j.1365-246X.2011.05007.x.

Wapenaar, K., Broggini, F., Slob, E., & Snieder, R., 2013. Three-dimensional single-sided Marchenko inverse scattering, data-driven focusing, Green's function retrieval, and their mutual relations. Physical Review Letters, 110(8), 084301. doi: 10.1103/PhysRevLett.110.084301.

Wapenaar, K., Thorbecke, J., van der Neut, J., Broggini, F., Slob, E., & Snieder, R., 2014b. Marchenko imaging. Geophysics, 79, WA39-WA57. doi: 10.1190/geo2013-0302.1.

Ziolkowski, A., Taylor, D. B., & Johnston, R. G. K., 1999. Marine seismic wavefield measurement to remove sea surface multiples, Geophysical Prospecting, 47, 841–870.
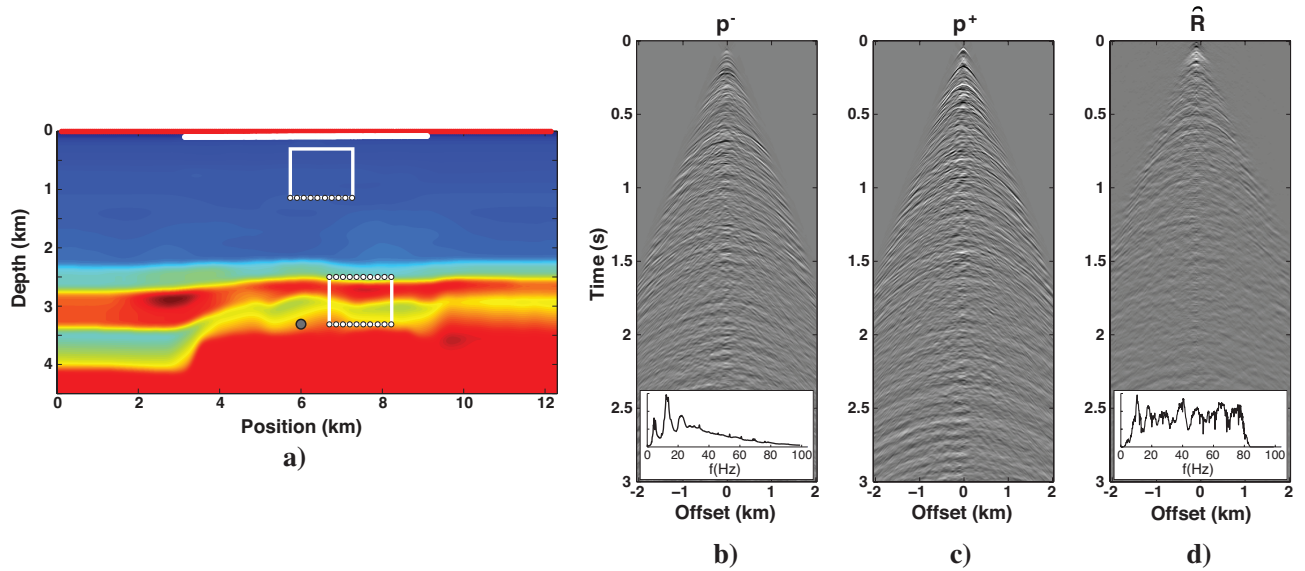
8. Figures

Figure 1 *a) Migration velocity model, source array at depth z_S=6 m (red line) and receiver array at z_R=90 m (white line) in the ocean-bottom cable acquisition. A grey dot represents the subsurface point where Marchenko fields shown in Figure 3 are computed using equations 3 and 1, while two white boxes indicate the target areas where Marchenko imaging is performed. Single common-shot gather of the b) up-going pressure data **p⁻**, c) down-going pressure data **p⁺**, and d) estimate of the reflection response **R̂**. Inserts in b) and d) show the average amplitude spectra of the gathers.*
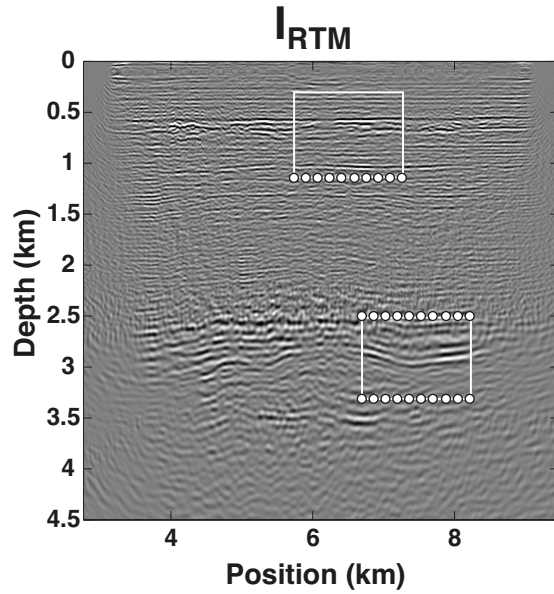
18

Figure 2 *Subsurface image obtained by applying standard RTM to the estimate of the ideal reflection response ($\hat{\mathbf{R}}$) shown in Figure 1d.*
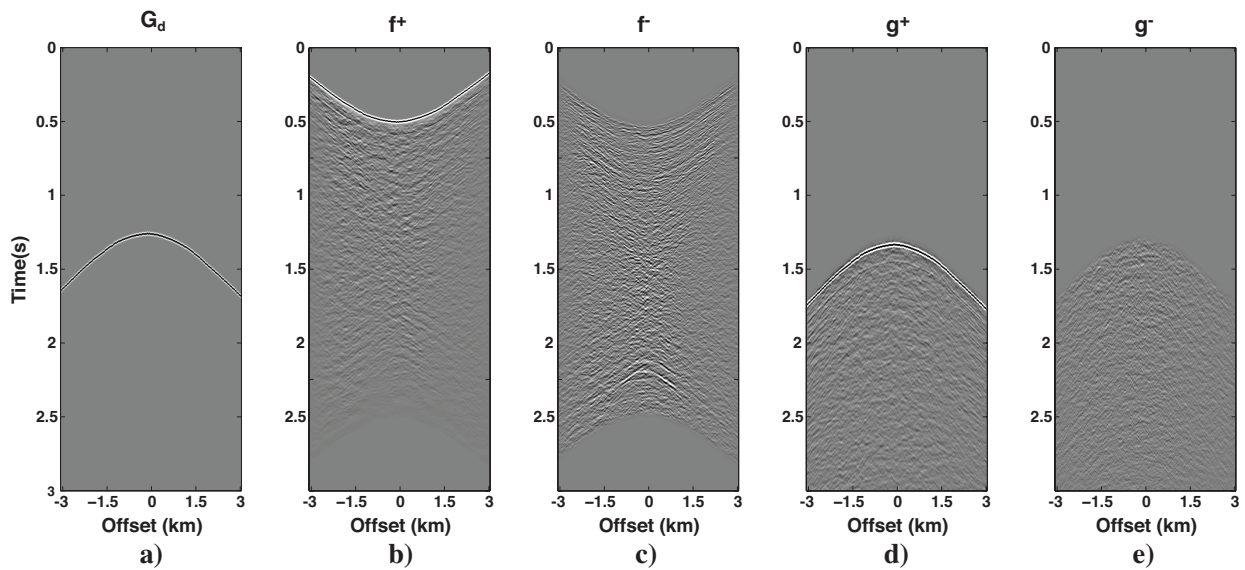

Figure 3 *Marchenko redatuming. a) Forward-modelled first arriving wave. b) Down- and c) up-going focusing functions, and d) down- and e) up-going redatumed fields at $\mathbf{x}_F$. All panels are displayed with 50% clipping of absolute amplitudes.*
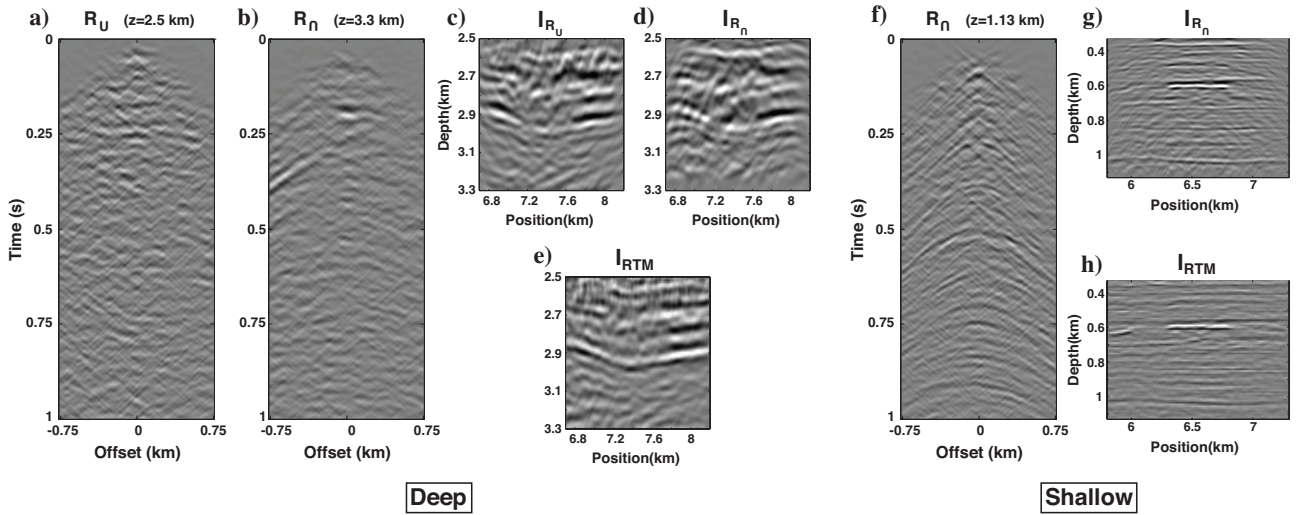
Figure 4 *Marchenko imaging. Multi-dimensional deconvolution estimates of a) reflection response from above* $\mathbf{R}_\cup$ *at depth level z=2.5 km, and b) reflection response from below* $\mathbf{R}_\cap$ *at depth level z=3.3 km. Images of the target zone from c) above and d) below, compared to that obtained from e) standard RTM of the reflection response* $\hat{\mathbf{R}}$*. f), g), and h) same as b), d), and e) for a shallower depth level (z=1.13 km).*
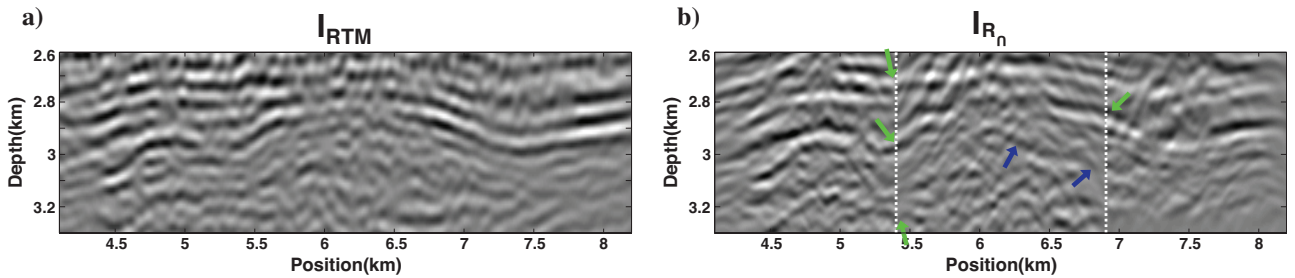

Figure 5 *Merging of Marchenko images. a) Standard RTM of the reflection response* $\hat{\mathbf{R}}$ *and b) Marchenko imaging from below of three different subsurface redatumed responses* $\mathbf{R}_\cap$ *(white dashed lines delimit the three images). Green arrows in b) indicate near-perfect continuity between images. Blue arrows in b) refer to a continuous structure revealed by Marchenko imaging that is not visible in the RTM image.*